JACS
JOURNAL OF THE AMERICAN CHEMICAL SOCIETY

pubs.acs.org/JACS

Article

Photochemical Identification of Auxiliary Severe Acute Respiratory Syndrome Coronavirus 2 Host Entry Factors Using μMap

Saori Suzuki,[#] Jacob B. Geri,[#] Steve D. Knutson,[#] Harris Bell-Temin, Tomokazu Tamura, David F. Fernández, Gabrielle H. Lovett, Nicholas A. Till, Brigitte L. Heller, Jinchao Guo, David W. C. MacMillan,* and Alexander Ploss*

Cite This: J. Am. Chem. Soc. 2022, 144, 16604−16611

Read Online

ACCESS | Metrics & More | Article Recommendations | Supporting Information

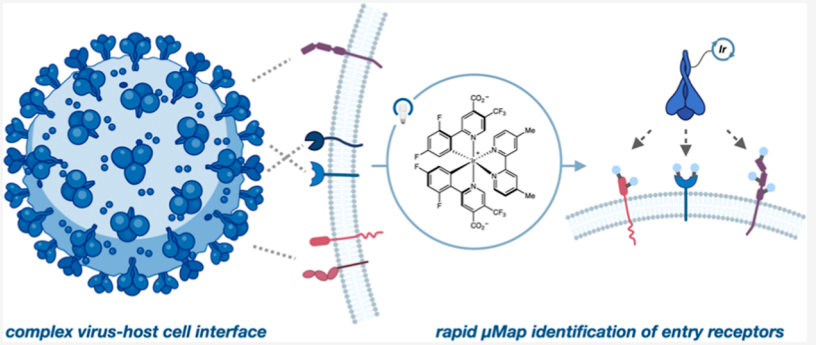

ABSTRACT: Severe acute respiratory syndrome coronavirus 2 (SARS-CoV-2), the infectious agent of the COVID-19 pandemic, remains a global medical problem. Angiotensin-converting enzyme 2 (*ACE2*) was identified as the primary viral entry receptor, and transmembrane serine protease 2 primes the spike protein for membrane fusion. However, *ACE2* expression is generally low and variable across tissues, suggesting that auxiliary receptors facilitate viral entry. Identifying these factors is critical for understanding SARS-Cov-2 pathophysiology and developing new countermeasures. However, profiling host−virus interactomes involves extensive genetic screening or complex computational predictions. Here, we leverage the photocatalytic proximity labeling platform μMap to rapidly profile the spike interactome in human cells and identify eight novel candidate receptors. We systemically validate their functionality in SARS-CoV-2 pseudoviral uptake assays with both Wuhan and Delta spike variants and show that dual expression of *ACE2* with either neuropilin-2, ephrin receptor A7, solute carrier family 6 member 15, or myelin and lymphocyte protein 2 significantly enhances viral uptake. Collectively, our data show that SARS-CoV-2 synergistically engages several host factors for cell entry and establishes μMap as a powerful tool for rapidly interrogating host−virus interactomes.

INTRODUCTION

Severe acute respiratory syndrome coronavirus 2 (SARS-CoV-2) is the etiologic agent of the COVID-19 pandemic. Identifying viral entry and replication factors is key for understanding and resolving outbreaks, and angiotensin-converting enzyme 2 (*ACE2*) has been identified as the obligate receptor for SARS-CoV and SARS-CoV-2.[1,2] Cleavage of the viral spike protein by the transmembrane serine protease 2 (*TMPRSS2*) also facilitates SARS-CoV-2 membrane fusion.[3−5] Although *ACE2* expression is higher in nasal epithelial cells, these levels decrease throughout the lower respiratory tract.[1,2] While this implies nasal initiation of infection, transition mechanisms to deep lung pathogenesis in severe COVID are unknown.[6,7] Similarly, COVID infections can rapidly progress throughout the body and cause multiple organ failure,[8] yet *ACE2* expression is low or variable beyond gastrointestinal and respiratory tracts.[9] Accordingly, it is likely that SARS-CoV-2 interacts with additional receptors, although viral entry outside of canonical pathways remains poorly characterized (Figure 1a).

Computational modeling of the receptor binding domain (RBD) has identified interactions with heparin sulfate for cell entry, and recent work has validated functional associations with C-type lectin receptors[10] and metabotropic glutamate receptor 2.[11] Additionally, results from two studies suggest that neuropilin-1 (*NRP1*) enhances *TMPRSS2*-mediated SARS-CoV-2 entry.[12,13] Although these studies elucidated additional viral entry routes, they also required extensive computational effort generated from crystal structures or validated hypotheses

Received: June 28, 2022
Published: September 1, 2022

https://doi.org/10.1021/jacs.2c06806
J. Am. Chem. Soc. 2022, 144, 16604−16611

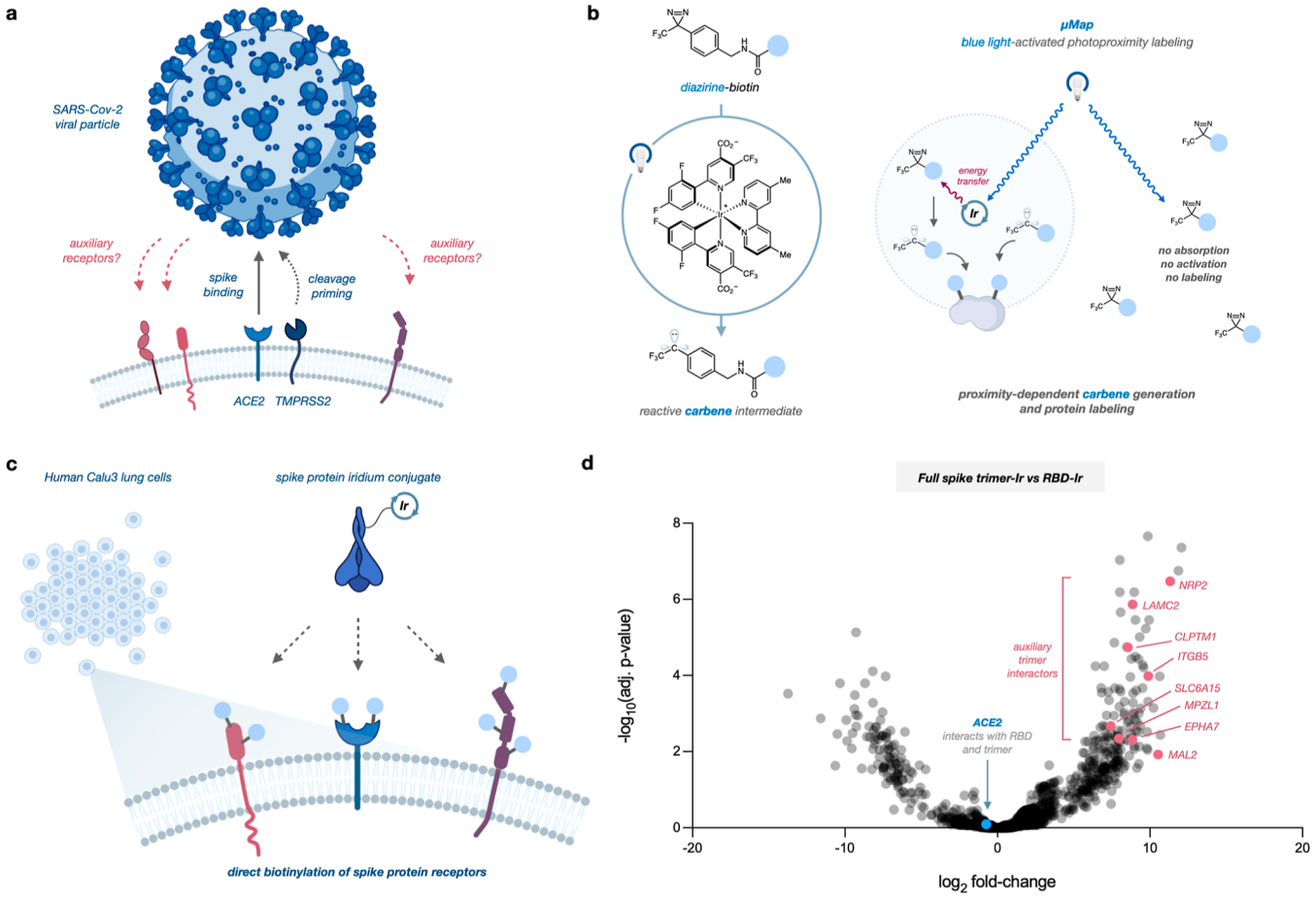

Figure 1. (a) SARS-Cov-2 utilizes *ACE2* and *TMPRSS2* for cell uptake, but additional entry factors are likely. (b) μMap photoproximity labeling via Ir photocatalysts that activate nearby diazirines into reactive carbenes. (c) Ir conjugation with SARS-Cov-2 spike protein enables rapid receptor identification. (d) Quantitative proteomics volcano plot of candidate cell−surface proteins after incubation of Ir-spike proteins with Calu-3 cells and photolabeling. Data set compares full-length spike protein against RBD. *ACE2* interacts with both constructs and is thus near zero enrichment.

from a priori evidence of known receptors. Genetic knock-out screens can reduce bias and allow identification of proviral proteins,[14] yet these campaigns involve extensive library optimization and require suitable systems for transfection and engineering. In contrast, proximity labeling has emerged as a versatile methodology for unbiased interrogation of protein interactions via catalytic tagging of spatially connected biomolecules.[15] APEX[16] and BioID[17] have found particular widespread application and have been recently utilized for investigating associations between SARS-Cov-2 viral components and intracellular host proteins. Although these studies demonstrated relevant interactions between the viral proteins and the host signal peptidase complex[18] as well as myosin heavy chain,[19] these platforms require genetic engineering to introduce proximity labeling components and are limited in both spatial control and labeling resolution. To circumvent these challenges and investigate the native cell−surface interactome with greater precision, we hypothesized that our recently developed photocatalytic proximity labeling method, μMap,[20] could directly profile the host−virus microenvironment and identify SARS-CoV-2 auxiliary receptors (Figure 1b,c). In contrast to peroxidase or biotin ligation strategies, μMap uses iridium (Ir) photocatalysts to convert nearby diazirines into carbenes via Dexter energy transfer and biotinylate proteins within ∼4 nm radius, offering high spatial and temporal control over labeling (Figure 1b).[20] This platform has been applied for small molecule target identification,[21] mapping chromatin reorganization events,[22] and rapidly profiling immunosynapse interactions.[20] Additionally, similar Ir-based photocatalytic proximity labeling strategies have also been recently developed for cataloging mitochondrial proteins in activated macrophages[23] and profiling surface proteins in breast cancer.[24] Rhodamine-based oxidation labeling has also provided new methodology for validating cell−surface microenvironments, underscoring the utility of light-mediated proximity labeling for interrogating cell−surface proteomes with high spatiotemporal precision.[25] Given this precedent, we sought to deploy μMap to identify novel receptors of the SARS-CoV-2 spike protein.

RESULTS AND DISCUSSION

As an initial test, we first synthesized recombinant RBD and full-length spike-Ir conjugates and attempted photolabeling on HEK293T cells overexpressing *ACE2* (Figure S1). Cells were incubated with spike-Ir conjugates and then washed, and photolabeling was initiated in a 250 μM biotin−diazirine solution under blue light irradiation. Compared with a free Ir control and parental 293T cells, we observed robust biotinylation of membrane proteins from trimer conjugates only in *ACE2*-expressing cells (Figure S2). Notably, RBD labeling produced few new bands beyond *ACE2* in these tests,

https://doi.org/10.1021/jacs.2c06806
J. Am. Chem. Soc. 2022, 144, 16604−16611

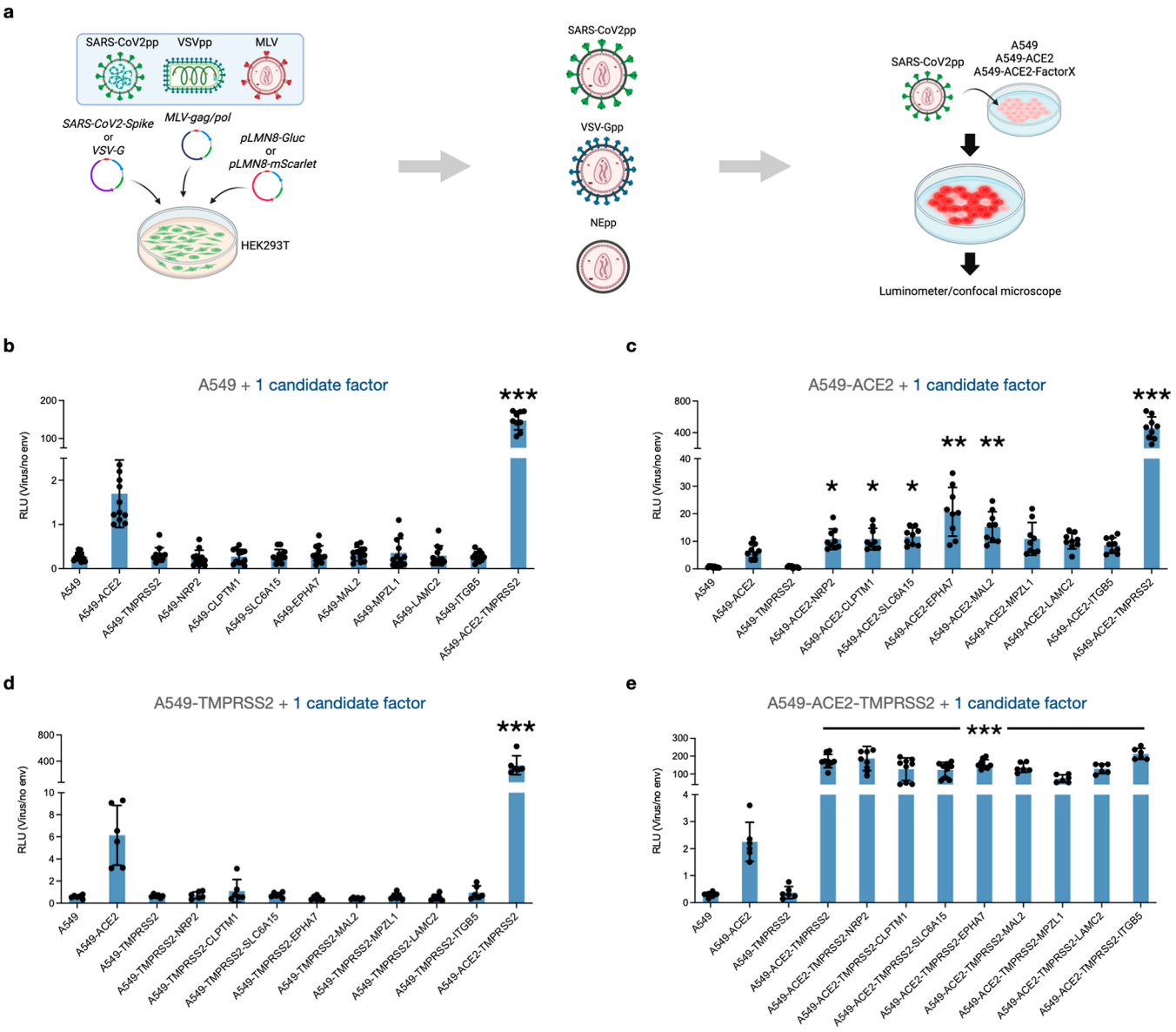

Figure 2. SARS-CoV-2 uptake is enhanced in cells expressing candidate receptors and *ACE2*. (a) Schematic for generating pseudoviral particles and infection. (b–e) Virus uptake into A549 cells expressing *ACE2*, *TMPRSS2*, and/or entry factor candidates. Entry was measured as relative luminescent signal (RLU) normalized against non-enveloped particle control. Data points represent mean ($n = 6$) and error bars denote standard deviation. Independent *t*-tests between *ACE2* and expression lines are indicated $^{*}p < 0.05$, $^{**}p < 0.01$, $^{***}p < 0.001$.

yet the spike trimer displayed extensive biotinylation, revealing the possibility of novel interactions.

To perform μMap analysis of the spike interactome in a native context, we identified Calu-3 human lung cells as they express both canonical entry factors *ACE2* and *TMPRSS2* (Figure S1) and have been previously utilized to study COVID pathophysiology.[1,2] We were also particularly interested in utilizing the full-length spike protein (~180 kDa), as the N-terminal domain bears epitopes of neutralizing antibodies, yet its functional interactions are still unknown,[26,27] suggesting that it binds other host factors. We executed our photolabeling workflow followed by membrane lysate isolation, streptavidin enrichment, and quantitative proteomic analysis. Compared against a free Ir control, *ACE2* was strongly enriched (Figure S3 and Table S1), recapitulating our initial feasibility test. To delineate auxiliary interactions between the smaller RBD (~50 kDa) and full spike, we also performed μMap with both conjugates and compared data sets. As expected, *ACE2* was not enriched as it binds both protein constructs, but we identified eight enriched membrane proteins as candidate receptors for the full spike (Figure 1d and Table S2). *TMPRSS2* was not observed in any of our data sets, which is unexpected given its known role as a canonical SARS-CoV-2 entry factor along with *ACE2*.[3−5] However, it is also known that the *TMPRSS2*-spike interaction is transient after cleavage, and given that μMap targeting of cell−surface proteins employs binding and several washing steps, we hypothesize that this contributed to lack of proteomic detection. Regardless, neuropilin-2 (*NRP2*) was highly enriched, and has high homology with *NRP1* which was reported to bind to the cleaved spike and facilitate SARS-CoV-2 entry.[12,13] Cleft lip and palate associated transmembrane protein 1 (*CLPTM1*) and ephrin receptor A7 (*EPHA7*) were also prioritized, the latter of which was reported as key for transmission of Kaposi's sarcoma-associated herpes virus and

https://doi.org/10.1021/jacs.2c06806
J. Am. Chem. Soc. 2022, 144, 16604−16611

rhesus monkey rhadinovirus.[28] We also identified myelin and lymphocyte protein 2 (*MAL2*), recently reported as a herpes simplex virus 1 co-factor in oligodendrocytes.[29] Solute carrier family 6 member 15 (*SLC6A15*), myelin protein zero-like protein 1 (*MPZL1*), laminin subunit gamma 2 (*LAMC2*), and integrin subunit beta 5 (*ITGB5*) were also noted as candidate receptors (Figure 1d and Table S2). *LAMC2* was intriguingly identified in a microarray study as a possible SARS-CoV-2 transmission factor.[30] Although these eight annotated candidate proteins are not the sole transmembrane proteins enriched in our data set (Figure 1d and Table S2), this group was selected due to their high enrichment and likelihood of interacting with the SARS-CoV-2 spike protein on the cell surface. Importantly, all candidates are known to be expressed in esophageal and respiratory tract tissues,[31] and so we next sought to functionally test these receptors for viral infection.

We first generated SARS-CoV-2 pseudovirus particles (SARS-CoV-2pp) encoding Gaussia luciferase as a quantifiable proxy (Figure 2a). In line with previous observations, expression of *ACE2* or *TMPRSS2* in HEK293T and A549 cells resulted in significant entry enhancement (Figure S4). We next constructed a panel of A549 cell lines to display various combinations of cell−surface candidate factors. Importantly, we transduced cells with bicistronic lentiviral cassettes containing a zsGreen reporter to enable fluorescence-activated cell sorting and standardized expression of each markers, and *ACE2* levels were similarly gated using antibody staining (Figure S5). For additional rigor, we also measured expression of respective genes in sorted cell lines via quantitative PCR and verified similar mRNA levels (Figure S6). We next infected these lines with SARS-Cov-2pp, and although A549 cells expressing *ACE2* and/or *TMPRSS2* exhibited significant increases in viral uptake compared to parental cells, display of individual candidate factors provided no viral uptake enhancement (Figure 2b). However, cells stably expressing *ACE2* along with individual factors exhibited significantly enhanced viral entry (Figure 2c). In particular, dual expression of *ACE2* with *NRP2*, *CLPTM1*, *SLC6A15*, *EPHA7*, or *MAL2* led to upward of ∼3-fold increases in viral uptake compared with cells only expressing *ACE2*, suggesting a synergistic cell entry mechanism. As expected, *TMPRSS2* conferred large uptake increases when expressed with *ACE2* (Figure 2b−e), yet no difference was observed in lines expressing *TMPRSS2* and each factor (Figure 2d) or in combination with *ACE2* and *TMPRSS2* (Figure 2e). We hypothesized that these differences may be masked by enzymatic luciferase-based detection, so to observe uptake in greater detail, we infected *ACE2*−*TMPRSS2* triple expression lines displaying the highest enhancement (*NRP2*, *SLC6A15*, *EPHA7*, and *MAL2*) with mScarlet reporter pseudoparticles (Figure 3). Quantifying individual populations via microscopy confirmed minimal entry in A549 cells as well as lines expressing only *ACE2*, but large enhancement was seen in *ACE2* lines simultaneously displaying *TMPRSS2* along with *NRP2*, *MAL2*, *EPHA7*, or *SLC6A15*. Non-enveloped viral controls showed no uptake (Figure S7), reflecting spike-mediated entry (Figure 3a,b). Together, these results confirm the importance of *ACE2* and *TMPRSS2* for SARS-Cov-2 entry, and we excitingly demonstrate that *NRP2*, *SLC6A15*, *EPHA7*, and *MAL2* significantly enhance viral uptake when expressed with *ACE2*.

Numerous SARS-CoV-2 variants have continued to emerge that are increasingly transmissible and/or less vulnerable to antibody neutralization. In particular, the Delta (B.1.617.2) variant that arose in India in late 2020 contains eight amino acid mutations from the original Wuhan spike (Figure 4a).[32] To test uptake with our identified receptors, we generated Delta SARS-CoV2-pp and repeated our luminescent entry

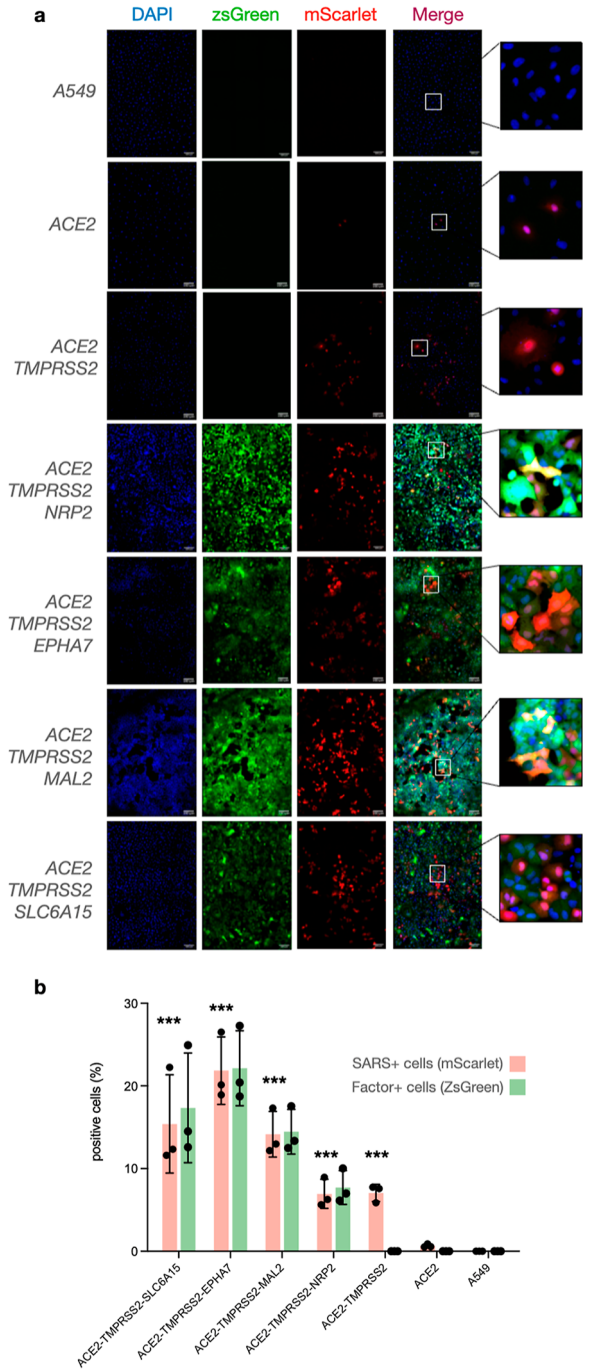

Figure 3. *NRP2*, *MAL2*, *EPHA7*, and *SLC6A15* significantly enhance SARS-Cov-2 entry. (a) A549 cells expressing various factors were infected with SARS-CoV-2pp encoding mScarlet, stained with DAPI (blue), and visualized using fluorescence microscopy for factor expression (szGreen) and viral uptake (red). Scale bar indicates 100 μm, and insets display zoomed-in regions of each image. (b) Entry quantification as percentage of red: (SARS positive)/(DAPI positive) and green: percentage of (SARS positive)/(factor positive). Data points represent mean from (n = 3), and error bars denote standard deviation. Independent t-tests of SARS+ values between *ACE2* and *ACE2*−*TMPRSS2* triple expression lines are indicated as significant (***$p < 0.001$).

https://doi.org/10.1021/jacs.2c06806
J. Am. Chem. Soc. 2022, 144, 16604−16611

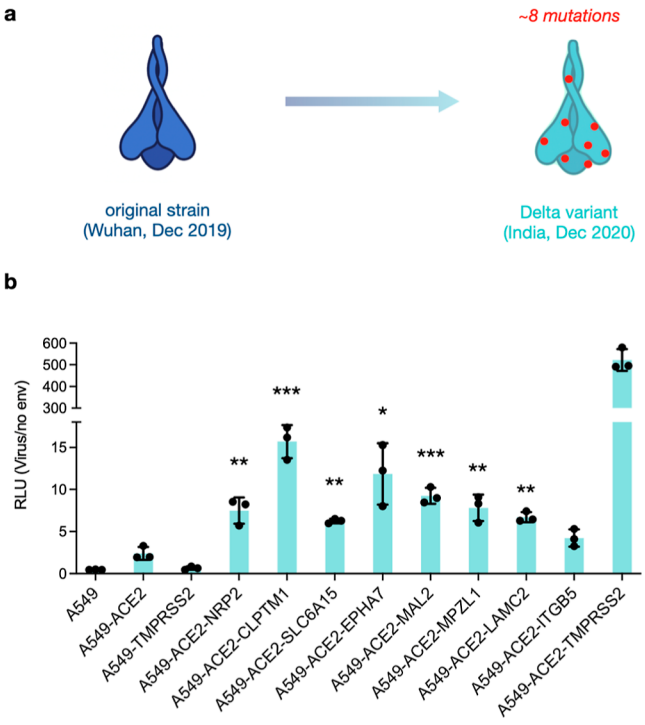

Figure 4. Candidate receptors enhance Delta variant spike-mediated uptake. (a) Delta variant spike harbors eight mutations compared to Wuhan strain. (b) Delta pseudovirus uptake in cells expressing *ACE2* and candidate factors. Entry was measured as relative luminescent signal (RLU) normalized against non-enveloped particle control. Data points represent mean (n = 3) and error bars denote standard deviation. Independent t-tests between *ACE2* and respective lines are indicated as significant $^{*}p < 0.05$, $^{**}p < 0.01$, $^{***}p < 0.001$.

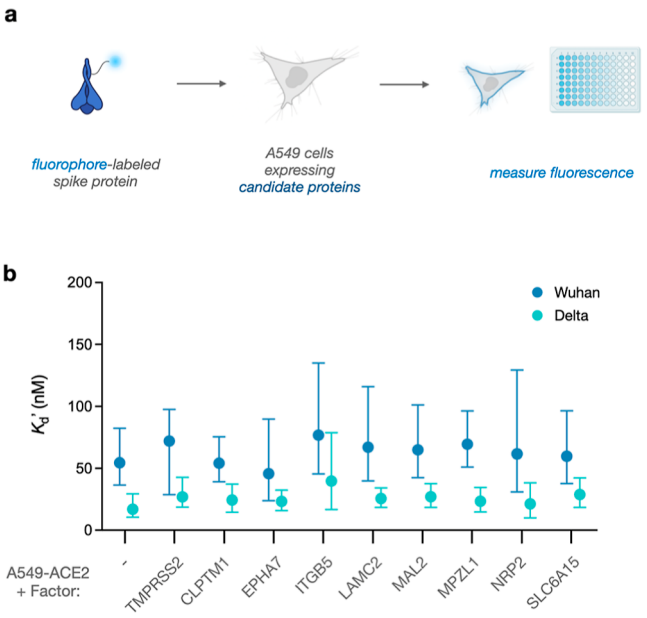

Figure 5. Candidate receptors do not enhance SARS-Cov-2 spike binding on human cells. (a) Schematic for testing binding affinity of spike protein and candidate factors. (b) Apparent dissociation constants (K'_d) for SARS-Cov-2 spike from Wuhan (blue) and Delta (green) strains toward cells expressing *ACE2* and various cell–surface proteins. Data points represent mean (n = 3), and error bars denote 95% confidence intervals.

assay and interestingly observed significant entry enhancement across all factors except for *ITGB5*, with upward of ∼5–7-fold increases in *ACE2–CLPTM1* and *ACE2–EPHA7* lines versus cells only expressing *ACE2* (Figure 4b). Conversely, the Wuhan strain only exhibited increased uptake in cell lines expressing both *ACE2* in combination with *NRP2*, *MAL2*, *EPHA7*, or *SLC6A15* (Figure 2c), suggesting that the higher transmissibility of the Delta variant is due in part to broader receptor tropism.

Lastly, we sought to probe whether candidate factors stably interact with SARS-Cov-2. Fluorophore-spike conjugates were generated, and each cell line was incubated with increasing amounts of the conjugate. After washing, fluorescence was measured to estimate remaining bound protein (Figure 5a). As expected, parental A549 cells displayed minimal interaction whereas cells expressing *ACE2* exhibited robust binding with low nM affinity (Figures S8 and 5b). Intriguingly, the Delta spike variant exhibited significantly enhanced binding affinity in all *ACE2*-expressing lines, in agreement with working hypotheses regarding its higher transmissibility (Figures S9 and 5b).[33] However, cell lines expressing each candidate displayed minimal binding, and dual expression with *ACE2* did not increase affinity compared with single expression of *ACE2* in either variant. Although we anticipated observing a binding enhancement, not all entry factors stably interact with the spike protein. In agreement with prior work, *TMPRSS2*-expressing cells did not stably bind (Figures S8 and S9), despite the significant impact of the protease on viral uptake.[1] Similarly, *NRP1* was found to enhance cell entry, yet binding interactions with SARS-Cov-2 were undetectable in analogous assays.[12] Although the candidate factors identified in this study functionally enhance uptake, our results suggest that interactions with the spike protein are transient, and synergistic associations between *ACE2* and a receptor ensemble likely contribute to spike binding and subsequent particle entry.

Understanding the molecular mechanisms of SARS-Cov-2 infection across human tissues is key to resolving the current pandemic and developing countermeasures for future outbreaks. Here, we show that photocatalytic proximity labeling using μMap is a rapid and powerful tool for interrogating critical receptors at the host–virus interface. We profile the Wuhan spike interactome and identify at least four proteins, *NRP2*, *MAL2*, *EPHA7*, and *SLC6A15*, as auxiliary SARS-Cov-2 entry receptors that significantly enhance uptake of both the original and Delta SARS-Cov-2 variants in human cells. The Omicron spike variant has now dominated global infections, and the molecular mechanisms of its high transmissibility and immune evasion remain poorly understood.[34,35] Ongoing research in our group seeks to expand this work into emerging variants across human cell types to delineate these complex interactions. Additionally, we observed many intracellular proteins that were enriched in our data sets (Figure 1d, Tables S1 and S2) that potentially interact with the SARS-CoV-2 spike protein. We hypothesize that these interactions are potentially resulting from internalized spike-Ir conjugates, and future efforts will validate and functionally investigate these potentially critical interactions. Moreover, we and the Rovis group have also recently reported red light-based strategies for photocatalyic proximity labeling,[36,37] and future efforts will deploy these platforms for studying host–virus interactions in complex in vivo environments. Together, this work demonstrates a powerful and generalizable methodology

https://doi.org/10.1021/jacs.2c06806
J. Am. Chem. Soc. 2022, 144, 16604–16611

for rapidly elucidating entry mechanisms for a variety of pathogens in diverse cellular settings.

■ ASSOCIATED CONTENT

Supporting Information

The Supporting Information is available free of charge at https://pubs.acs.org/doi/10.1021/jacs.2c06806.

Proteomic data sets (XLSX)

Experimental procedures and supplementary figures (PDF)

■ AUTHOR INFORMATION

Corresponding Authors

David W. C. MacMillan − *Department of Chemistry, Princeton University, Princeton, New Jersey 08544, United States; Merck Center for Catalysis at Princeton University, Princeton, New Jersey 08544, United States;* orcid.org/0000-0001-6447-0587; Email: dmacmill@princeton.edu

Alexander Ploss − *Department of Molecular Biology, Princeton University, Princeton, New Jersey 08544, United States;* orcid.org/0000-0001-9322-7252; Email: aploss@princeton.edu

Authors

Saori Suzuki − *Department of Molecular Biology, Princeton University, Princeton, New Jersey 08544, United States;* orcid.org/0000-0001-5233-6604

Jacob B. Geri − *Department of Chemistry, Princeton University, Princeton, New Jersey 08544, United States*

Steve D. Knutson − *Department of Chemistry, Princeton University, Princeton, New Jersey 08544, United States*

Harris Bell-Temin − *Bristol Myers Squibb, Princeton, New Jersey 08540, United States*

Tomokazu Tamura − *Department of Molecular Biology, Princeton University, Princeton, New Jersey 08544, United States*

David F. Fernández − *Department of Chemistry, Princeton University, Princeton, New Jersey 08544, United States;* orcid.org/0000-0003-3482-0894

Gabrielle H. Lovett − *Department of Chemistry, Princeton University, Princeton, New Jersey 08544, United States*

Nicholas A. Till − *Department of Chemistry, Princeton University, Princeton, New Jersey 08544, United States;* orcid.org/0000-0003-2421-7186

Brigitte L. Heller − *Department of Molecular Biology, Princeton University, Princeton, New Jersey 08544, United States*

Jinchao Guo − *Department of Molecular Biology, Princeton University, Princeton, New Jersey 08544, United States*

Complete contact information is available at: https://pubs.acs.org/10.1021/jacs.2c06806

Author Contributions

#S.S., J.B.G., and S.D.K. contributed equally. The manuscript was written through contributions of all authors. All authors have given approval to the final version of the manuscript.

Funding

This study was funded in part by grants from the National Institutes of Health (R01AI138797, R01AI107301, R01AI146917, and R01AI153236 to A.P.), a Burroughs Wellcome Fund Award for Investigators in Pathogenesis (101539 to A.P.), and Princeton COVID-19 research funds through the Office of the Dean for Research and a component of the National Institutes of Health (NIH) under award number UL1TR003017 (to A.P.). This work was also funded by the NIH National Institute of General Medical Sciences (R35-GM134897-02). S.D.K. acknowledges the NIH for a postdoctoral fellowship (1F32GM142206-01). The Molecular Biology Flow Cytometry Resource Facility is partially supported by the Cancer Institute of New Jersey Cancer Center Support grant (P30CA072720). The content is solely the responsibility of the authors and does not necessarily represent the official views of the National Institutes of Health.

Notes

The authors declare no competing financial interest.

■ ACKNOWLEDGMENTS

This work was supported by kind gifts from Merck, BMS, Pfizer, Janssen, Genentech, and Eli Lilly. We also acknowledge the Princeton Catalysis Initiative for supporting this work. The authors thank Saw Kyin and Henry H. Shwe at the Princeton Proteomics Facility. We also thank Mohsan Saeed (Boston University) for providing A549-ACE2/TMPRSS2 cells,pLOC-ACE2-PuroR, and SARS-CoV2-S_B.1.1.529_codon optimized plasmid and Celeste Nelson for providing the Calu-3, BEAS-2B, and NuLi-1 cell lines. We are grateful to Christina DeCoste and Katherine Rittenbach of the Flow Cytometry Resource Facility at Princeton University for their assistance in the planning and execution of all flow cytometry experiments. We would also like to thank Gary S. Laevsky and Sha Wang of the Confocal Imaging Facility, a Nikon Center of Excellence, in the Department of Molecular Biology at Princeton University for instrument use and technical advice.

■ REFERENCES

(1) Hoffmann, M.; Kleine-Weber, H.; Schroeder, S.; Krüger, N.; Herrler, T.; Erichsen, S.; Schiergens, T. S.; Herrler, G.; Wu, N. H.; Nitsche, A.; et al. SARS-CoV-2 Cell Entry Depends on ACE2 and TMPRSS2 and Is Blocked by a Clinically Proven Protease Inhibitor. *Cell* **2020**, *181*, 271−280.

(2) Li, W.; Moore, M. J.; Vasilieva, N.; Sui, J.; Wong, S. K.; Berne, M. A.; Somasundaran, M.; Sullivan, J. L.; Luzuriaga, K.; Greenough, T. C.; et al. Angiotensin-converting enzyme 2 is a functional receptor for the SARS coronavirus. *Nature* **2003**, *426*, 450−454.

(3) Glowacka, I.; Bertram, S.; Müller, M. A.; Allen, P.; Soilleux, E.; Pfefferle, S.; Steffen, I.; Tsegaye, T. S.; He, Y.; Gnirss, K.; Niemeyer, D.; Schneider, H.; Drosten, C.; Pöhlmann, S. Evidence that TMPRSS2 activates the severe acute respiratory syndrome coronavirus spike protein for membrane fusion and reduces viral control by the humoral immune response. *J. Virol.* **2011**, *85*, 4122−4134.

(4) Matsuyama, S.; Nagata, N.; Shirato, K.; Kawase, M.; Takeda, M.; Taguchi, F. Efficient activation of the severe acute respiratory syndrome coronavirus spike protein by the transmembrane protease TMPRSS2. *J. Virol.* **2010**, *84*, 12658−12664.

(5) Shulla, A.; Heald-Sargent, T.; Subramanya, G.; Zhao, J.; Perlman, S.; Gallagher, T. A transmembrane serine protease is linked to the severe acute respiratory syndrome coronavirus receptor and activates virus entry. *J. Virol.* **2011**, *85*, 873−882.

(6) Hou, Y. J.; Okuda, K.; Edwards, C. E.; Martinez, D. R.; Asakura, T.; Dinnon, K. H., 3rd; Kato, T.; Lee, R. E.; Yount, B. L.; Mascenik, T. M.; et al. SARS-CoV-2 Reverse Genetics Reveals a Variable Infection Gradient in the Respiratory Tract. *Cell* **2020**, *182*, 429−446.

(7) Ahn, J. H.; Kim, J.; Hong, S. P.; Choi, S. Y.; Yang, M. J.; Ju, Y. S.; Kim, Y. T.; Kim, H. M.; Rahman, M. D. T.; Chung, M. K.; et al. Nasal ciliated cells are primary targets for SARS-CoV-2 replication in the early stage of COVID-19. *J. Clin. Invest.* **2021**, *131*, No. e148517.

(8) Delorey, T. M.; Ziegler, C. G.; Heimberg, G.; Normand, R.; Yang, Y.; Segerstolpe, Å.; Abbondanza, D.; Fleming, S. J.; Subramanian, A.; Montoro, D. T.; Jagadeesh, K. A.; Dey, K. K.; Sen, P.; Slyper, M.; Pita-Juárez, Y. H.; Phillips, D.; Biermann, J.; Bloom-Ackermann, Z.; Barkas, N.; Ganna, A.; Gomez, J.; Melms, J. C.; Katsyv, I.; Normandin, E.; Naderi, P.; Popov, Y. V.; Raju, S. S.; Niezen, S.; Tsai, L. T.-Y.; Siddle, K. J.; Sud, M.; Tran, V. M.; Vellarikkal, S. K.; Wang, Y.; Amir-Zilberstein, L.; Atri, D. S.; Beechem, J.; Brook, O. R.; Chen, J.; Divakar, P.; Dorceus, P.; Engreitz, J. M.; Essene, A.; Fitzgerald, D. M.; Fropf, R.; Gazal, S.; Gould, J.; Grzyb, J.; Harvey, T.; Hecht, J.; Hether, T.; Jané-Valbuena, J.; Leney-Greene, M.; Ma, H.; McCabe, C.; McLoughlin, D. E.; Miller, E. M.; Muus, C.; Niemi, M.; Padera, R.; Pan, L.; Pant, D.; Pe'er, C.; Pfiffner-Borges, J.; Pinto, C. J.; Plaisted, J.; Reeves, J.; Ross, M.; Rudy, M.; Rueckert, E. H.; Siciliano, M.; Sturm, A.; Todres, E.; Waghray, A.; Warren, S.; Zhang, S.; Zollinger, D. R.; Cosimi, L.; Gupta, R. M.; Hacohen, N.; Hibshoosh, H.; Hide, W.; Price, A. L.; Rajagopal, J.; Tata, P. R.; Riedel, S.; Szabo, G.; Tickle, T. L.; Ellinor, P. T.; Hung, D.; Sabeti, P. C.; Novak, R.; Rogers, R.; Ingber, D. E.; Jiang, Z. G.; Juric, D.; Babadi, M.; Farhi, S. L.; Izar, B.; Stone, J. R.; Vlachos, I. S.; Solomon, I. H.; Ashenberg, O.; Porter, C. B. M.; Li, B.; Shalek, A. K.; Villani, A.-C.; Rozenblatt-Rosen, O.; Regev, A. COVID-19 tissue atlases reveal SARS-CoV-2 pathology and cellular targets. *Nature* **2021**, *595*, 107−113.

(9) Hikmet, F.; Méar, L.; Edvinsson, Å.; Micke, P.; Uhlén, M.; Lindskog, C. The protein expression profile of ACE2 in human tissues. *Mol. Syst. Biol.* **2020**, *16*, No. e9610.

(10) Thépaut, M.; Luczkowiak, J.; Vivès, C.; Labiod, N.; Bally, I.; Lasala, F.; Grimoire, Y.; Fenel, D.; Sattin, S.; Thielens, N.; Schoehn, G.; Bernardi, A.; Delgado, R.; Fieschi, F. DC/L-SIGN recognition of spike glycoprotein promotes SARS-CoV-2 trans-infection and can be inhibited by a glycomimetic antagonist. *PLoS Pathog.* **2021**, *17*, No. e1009576.

(11) Wang, J.; Yang, G.; Wang, X.; Wen, Z.; Shuai, L.; Luo, J.; Wang, C.; Sun, Z.; Liu, R.; Ge, J. SARS-CoV-2 uses metabotropic glutamate receptor subtype 2 as an internalization factor to infect cells. *Cell Discovery* **2021**, *7*, 119.

(12) Daly, J. L.; Simonetti, B.; Klein, K.; Chen, K. E.; Williamson, M. K.; Antón-Plágaro, C.; Shoemark, D. K.; Simón-Gracia, L.; Bauer, M.; Hollandi, R.; et al. Neuropilin-1 is a host factor for SARS-CoV-2 infection. *Science* **2020**, *370*, 861−865.

(13) Cantuti-Castelvetri, L.; Ojha, R.; Pedro, L. D.; Djannatian, M.; Franz, J.; Kuivanen, S.; van der Meer, F.; Kallio, K.; Kaya, T.; Anastasina, M.; et al. Neuropilin-1 facilitates SARS-CoV-2 cell entry and infectivity. *Science* **2020**, *370*, 856−860.

(14) Baggen, J.; Persoons, L.; Vanstreels, E.; Jansen, S.; Van Looveren, D.; Boeckx, B.; Geudens, V.; De Man, J.; Jochmans, D.; Wauters, J.; Wauters, E.; Vanaudenaerde, B. M.; Lambrechts, D.; Neyts, J.; Dallmeier, K.; Thibaut, H. J.; Jacquemyn, M.; Maes, P.; Daelemans, D. Genome-wide CRISPR screening identifies TMEM106B as a proviral host factor for SARS-CoV-2. *Nat. Genet.* **2021**, *53*, 435−444.

(15) Qin, W.; Cho, K. F.; Cavanagh, P. E.; Ting, A. Y. Deciphering molecular interactions by proximity labeling. *Nat. Methods* **2021**, *18*, 133−143.

(16) Lam, S. S.; Martell, J. D.; Kamer, K. J.; Deerinck, T. J.; Ellisman, M. H.; Mootha, V. K.; Ting, A. Y. Directed evolution of APEX2 for electron microscopy and proximity labeling. *Nat. Methods* **2015**, *12*, 51−54.

(17) Roux, K. J.; Kim, D. I.; Raida, M.; Burke, B. A promiscuous biotin ligase fusion protein identifies proximal and interacting proteins in mammalian cells. *J. Cell Biol.* **2012**, *196*, 801−810.

(18) Chen, Z.; Wang, C.; Feng, X.; Nie, L.; Tang, M.; Zhang, H.; Xiong, Y.; Swisher, S. K.; Srivastava, M.; Chen, J. Interactomes of SARS-CoV-2 and human coronaviruses reveal host factors potentially affecting pathogenesis. *EMBO J.* **2021**, *40*, No. e107776.

(19) Chen, J.; Fan, J.; Chen, Z.; Zhang, M.; Peng, H.; Liu, J.; Ding, L.; Liu, M.; Zhao, C.; Zhao, P.; Zhang, S.; Zhang, X.; Xu, J. Nonmuscle myosin heavy chain IIA facilitates SARS-CoV-2 infection in human pulmonary cells. *Proc. Natl. Acad. Sci.* **2021**, *118*, No. e2111011118.

(20) Geri, J. B.; Oakley, J. V.; Reyes-Robles, T.; Wang, T.; McCarver, S. J.; White, C. H.; Rodriguez-Rivera, F. P.; Parker, D. L., Jr.; Hett, E. C.; Fadeyi, O. O.; Oslund, R. C.; MacMillan, D. W. C. Microenvironment mapping via Dexter energy transfer on immune cells. *Science* **2020**, *367*, 1091−1097.

(21) Trowbridge, A. D.; Seath, C. P.; Rodriguez-Rivera, F. P.; Li, B. X.; Dul, B. E.; Schwaid, A. G.; Geri, J. B.; Oakley, J. V.; Fadeyi, O. O.; Oslund, R. C.; Ryu, K. A.; White, C.; Reyes-Robles, T.; Tawa, P.; Parker, D. L.; MacMillan, D. W. C. Small molecule photocatalysis enables drug target identification via energy transfer. *bioRxiv* **2021**, DOI: 10.1101/2021.08.02.454797. accessed (08-01-2022)

(22) Seath, C. P.; Burton, A. J.; MacMillan, D. W.; Muir, T. W. Tracking chromatin state changes using μMap photo-proximity labeling. *bioRxiv* **2021**, DOI: 10.1101/2021.09.28.462236. accessed (08-01-2022)

(23) Huang, Z.; Liu, Z.; Xie, X.; Zeng, R.; Chen, Z.; Kong, L.; Fan, X.; Chen, P. R. Bioorthogonal photocatalytic Decaging-enabled mitochondrial proteomics. *J. Am. Chem. Soc.* **2021**, *143*, 18714−18720.

(24) Liu, Z.; Xie, X.; Huang, Z.; Lin, F.; Liu, S.; Chen, Z.; Qin, S.; Fan, X.; Chen, P. R. Spatially resolved cell tagging and surfaceome labeling via targeted photocatalytic decaging. *Chem* **2022**, *8*, 2179−2191.

(25) Müller, M.; Gräbnitz, F.; Barandun, N.; Shen, Y.; Wendt, F.; Steiner, S. N.; Severin, Y.; Vetterli, S. U.; Mondal, M.; Prudent, J. R. Light-mediated discovery of surfaceome nanoscale organization and intercellular receptor interaction networks. *Nat. Commun.* **2021**, *12*, 7036.

(26) Liu, L.; Wang, P.; Nair, M. S.; Yu, J.; Rapp, M.; Wang, Q.; Luo, Y.; Chan, J. F.; Sahi, V.; Figueroa, A.; et al. Potent neutralizing antibodies against multiple epitopes on SARS-CoV-2 spike. *Nature* **2020**, *584*, 450−456.

(27) Chi, X.; Yan, R.; Zhang, J.; Zhang, G.; Zhang, Y.; Hao, M.; Zhang, Z.; Fan, P.; Dong, Y.; Yang, Y.; et al. A neutralizing human antibody binds to the N-terminal domain of the Spike protein of SARS-CoV-2. *Science* **2020**, *369*, 650−655.

(28) Großkopf, A. K.; Schlagowski, S.; Hörnich, B. F.; Fricke, T.; Desrosiers, R. C.; Hahn, A. S. EphA7 Functions as Receptor on BJAB Cells for Cell-to-Cell Transmission of the Kaposi's Sarcoma-Associated Herpesvirus and for Cell-Free Infection by the Related Rhesus Monkey Rhadinovirus. *J. Virol.* **2019**, *93*, No. e00064-19.

(29) López-Guerrero, J. A.; de la Nuez, C.; Praena, B.; Sánchez-León, E.; Krummenacher, C.; Bello-MoralesHerpes, R. Simplex Virus 1 Spread in Oligodendrocytic Cells Is Highly Dependent on MAL Proteolipid. *J. Virol.* **2020**, *94*, No. e01739-19.

(30) Basu, A.; Sarkar, A.; Maulik, U. Study of cell to cell transmission of SARS CoV2 virus particle using gene network from microarray data. *bioRxiv* **2020**, DOI: 10.1101/2020.05.26.116780. accessed (08-01-2022)

(31) Consortium, G. The Genotype-Tissue Expression (GTEx) pilot analysis: multitissue gene regulation in humans. *Science* **2015**, *348*, 648−660.

(32) Liu, Y.; Liu, J.; Johnson, B. A.; Xia, H.; Ku, Z.; Schindewolf, C.; Widen, S. G.; An, Z.; Weaver, S. C.; Menachery, V. D.; Xie, X.; Shi, P.-Y. Delta spike P681R mutation enhances SARS-CoV-2 fitness over Alpha variant. *Cell Rep.* **2022**, *39*, 110829.

(33) Wu, L.; Zhou, L.; Mo, M.; Liu, T.; Wu, C.; Gong, C.; Lu, K.; Gong, L.; Zhu, W.; Xu, Z. SARS-CoV-2 Omicron RBD shows weaker binding affinity than the currently dominant Delta variant to human ACE2. *Signal Transduction Targeted Ther.* **2022**, *7*, 8.

(34) Hui, K. P.; Ho, J. C.; Cheung, M.-c.; Ng, K.-c.; Ching, R. H.; Lai, K.-l.; Kam, T. T.; Gu, H.; Sit, K.-Y.; Hsin, M. K.; Au, T. W. K.; Poon, L. L. M.; Peiris, M.; Nicholls, J. M.; Chan, M. C. W. SARS-CoV-2 Omicron variant replication in human bronchus and lung ex vivo. *Nature* **2022**, *603*, 715−720.

(35) Liu, L.; Iketani, S.; Guo, Y.; Chan, J. F.-W.; Wang, M.; Liu, L.; Luo, Y.; Chu, H.; Huang, Y.; Nair, M. S.; Yu, J.; Chik, K. K.-H.; Yuen,

T. T.-T.; Yoon, C.; To, K. K.-W.; Chen, H.; Yin, M. T.; Sobieszczyk, M. E.; Huang, Y.; Wang, H. H.; Sheng, Z.; Yuen, K.-Y.; Ho, D. D. Striking antibody evasion manifested by the Omicron variant of SARS-CoV-2. *Nature* **2022**, *602*, 676−681.

(36) Buksh, B. F.; Knutson, S. D.; Oakley, J. V.; Bissonnette, N. B.; Oblinsky, D. G.; Schwoerer, M. P.; Seath, C. P.; Geri, J. B.; Rodriguez-Rivera, F. P.; Parker, D. L.; Scholes, G. D.; Ploss, A.; MacMillan, D. W. C. μMap-Red: Proximity Labeling by Red Light Photocatalysis. *J. Am. Chem. Soc.* **2022**, *144*, 6154−6162.

(37) Tay, N.; Ryu, K. A.; Weber, J.; Olow, A.; Reichman, D.; Oslund, R.; Fadeyi, O.; Rovis, T. Targeted Activation in Localized Protein Environments via Deep Red Photoredox Catalysis. *ChemRxiv* **2021**, DOI: 10.26434/chemrxiv-2021-x9bjv. accessed (08-01-2022)

https://doi.org/10.1021/jacs.2c06806
J. Am. Chem. Soc. 2022, 144, 16604−16611